Design of Scannable Non-uniform Planar Array Structure for Maximum Side-Lobe Reduction

Ji-Hoon Bae, Kyung-Tae Kim, Cheol-Sig Pyo, and Jong-Suk Chae

ABSTRACT—In this letter, we propose a novel design scheme for an optimal non-uniform planar array geometry in view of maximum side-lobe reduction. This is implemented by a thinned array using a genetic algorithm. We show that the proposed method can maintain a low side-lobe level without pattern distortion during beam steering.

Keywords—Array antenna, planar array, genetic algorithm, side-lobe reduction.

I. Introduction

In the area of antenna array pattern synthesis, a non-uniformly spaced array (NUSA) can successfully achieve a low side-lobe level (SLL) by optimally adjusting the positions of the elements with uniform excitations [1]-[3]. A useful methodology for this synthesis field is the use of the thinned array theory [4]. However, in the NUSA, the array geometry may cause the outer SLL to increase, especially when the main beam direction is steered [1]. Therefore, undesirable large side-lobes greater than the first SLL can be seen within the visible region of $-90°\leq\theta\leq 90°$ when the main beam is scanned. Recently, we proposed a pattern synthesis method of a non-uniformly spaced linear array (NUSLA) using the Gauss-Newton algorithm [5]. A NUSLA designed by the proposed method can reduce both the inner side-lobes and outer side-lobes, simultaneously, while the beam direction is steered. On the basis of a NUSLA, the purpose of this letter is to find the optimal non-uniformly spaced planar array (NUSPA) structure, while maintaining a low SLL without pattern distortion during beam steering. Our approach makes use of the thinned array theory combined with our proposed NUSLA technique, while under certain constraints. The proposed method can also be applied to any array antenna structure [6]. In the following section, a pattern synthesis method for the design of an optimal NUSPA is presented in detail.

Manuscript received May 12, 2003; revised Oct. 15, 2003.

Ji-Hoon Bae (phone: +82 42 860 1363, email: baejh@etri.re.kr), Cheol-Sig Pyo (email: cspyo@etri.re.kr), and Jong-Suk Chae (email: jschae@etri.re.kr) are with Digital Broadcasting Research Division, ETRI, Daejeon, Korea.

Kyung-Tae Kim (email: juniorf@yumail.ac.kr) is with Division of Electrical Engineering and Computer Science, Yeungnam University, Kyungpook, Korea.

II. Problem Formulation

In order to generate a two-dimensional (2-D) planar grid of non-uniform spacing, the optimized NUSLA, with an odd number N of elements obtained by [5], is extended to a 2-D rectangular lattice. Its array pattern can be described as follows:

$$p_{nu}(u,v)=\frac{1}{N^2}\left[2\sum_{n=1}^{M}\cos(\kappa d_n^x\cdot(u-u_0))+1\right]\times\left[2\sum_{m=1}^{M}\cos(\kappa d_m^y\cdot(v-v_0))+1\right], \tag{1}$$

where κ is a free space constant, dx is the uniform element spacing in the x-axis, $u=\sin\theta\cos\phi$, $v=\sin\theta\sin\phi$, $u_0=\sin\theta_0\cos\phi_0$, $v_0=\sin\theta_0\sin\phi_0$, e_n^x is the optimized fractional change obtained from the uniform array element positions in the x-axis, $d_n^x=(n+e_n^x)dx$, $d_m^y=(m+e_m^y)dy$, $e_l^y=e_l^x$ $(l=1,\cdots,M)$, $dy=dx$, and M is given by $(N-1)/2$.

III. Non-Uniform Planar Array Pattern Synthesis

In this section, the thinned array theory using a genetic algorithm (GA) is applied to a modification of the NUSPA structure of (1). Consider a linear array pattern in (1) [5], which is similar to the Fourier series expression for an arbitrary real-valued function. If we define an array frequency, $w_n = 2\pi n \cdot dx \sin\theta$, the lowest array frequency can be associated with the center array element, and the higher order array frequencies with the outer array elements [7]. When an arbitrary real-valued function is composed of both slowly and rapidly varying functions, the higher frequencies may determine the higher variations of the function. Therefore, the SLL of the linear array may be more sensitive to the adjustment of components associated with the high order array frequencies. The concept of the array frequency of the linear array can be extended to a 2-D planar array problem. Cutting some elements off the corners can provide a greater reduction of the maximum SLL (MSLL) than the rectangular arrangement [2]. Therefore, we consider only the outer elements located in Region (A) and (B) belonging to the first quadrant, as shown in Fig. 1, to construct an optimal array geometry.

First, some of the corner elements from the above NUSPA of (1) are eliminated until the largest reduction of the MSLL is achieved. The resulting NUSPA is used as an initial array geometry. In the result, the GA search boundary can be determined if the elements of the corners are initially turned off (black), as shown in Fig. 1. Next, some elements in the outer regions of the initial NUSPA are optimally removed using the GA. In addition, we further assume that the outer elements of (B) also have the same arrangement as those of (A). The smart initial guess and the above constraint can provide a fast convergence to the optimal solution, minimizing computational complexity.

The resulting NUSPA pattern can be written as (2), where A^a_{mn} and A^b_{mn} are amplitude weights of elements (1 or 0), and M, Q, and R are defined in Fig. 1. $A^a_{mn}=1$ represents the element status as "on," whereas $A^a_{mn}=0$ represents "off." A^b_{mn} can be determined by A^a_{mn} due to their symmetric distributions. A chromosome is represented by a single one-dimensional (1-D) binary string, ordering the 2-D element status, A^a_{mn} within the genetic search region, into a 1-D row vector array. Namely, to form the 1-D binary string, the transpose of each column vector of A^a_{mn} is placed side by side. The cost function C to evaluate the fitness value, where θ is in the side-lobe region and ϕ is between 0° and 180°, is defined as follows:

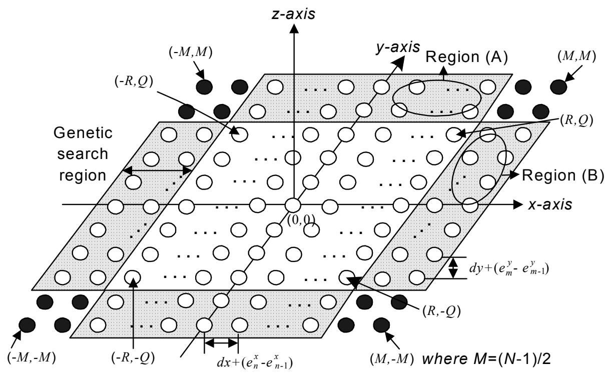

Fig. 1. Initial NUSPA geometry.

$$C = \max_{SLL}\left\{20\log\left(\left|p_{nu}\right|\right)\right\}. \tag{3}$$

The synthesis procedure for the NUSPA is summarized as follows:

Step 1: The optimized NUSLA is extended to a 2-D rectangular array, and some elements of the corner are eliminated to obtain an initial NUSPA.

Step 2: Generate an initial population for A^a_{mn} which represents a chromosome.

Step 3: Calculate the MSLL using (3).

Step 4: Rank the chromosomes from best to worst, according to their fitness values obtained by Step 3, and discard the bottom 50%.

Step 5: Create new offspring settings from the selected top 50% using the crossover operator.

Step 6: The best individual is excluded in the next process of mutation.

Step 7: Mutate the new offspring based on the probability of mutation.

Step 8: Repeat steps 2 to 7 until the fitness value C is less than a pre-defined threshold value.

$$\begin{aligned} p_{nu} = {} & \frac{1}{N^2}\left[2\sum_{n=1}^{R}\cos(\kappa d^x_n\cdot(u-u_0))+1\right]\cdot\left[2\sum_{m=1}^{Q}\cos(\kappa d^y_m\cdot(v-v_0))+1\right] \\ & +\frac{1}{N^2}\left(4\sum_{m=Q+1}^{M}\sum_{n=1}^{R}\left\{A^a_{mn}\cdot\cos(\kappa d^y_m\cdot(v-v_0))\cdot\cos(\kappa d^x_n\cdot(u-u_0))\right\}+2\sum_{m=Q+1}^{M}\cos(\kappa d^y_m\cdot(v-v_0))\right) \\ & +\frac{1}{N^2}\left(4\sum_{m=1}^{Q}\sum_{n=R+1}^{M}\left\{A^b_{mn}\cdot\cos(\kappa d^y_m\cdot(v-v_0))\cdot\cos(\kappa d^x_n\cdot(u-u_0))\right\}+2\sum_{n=R+1}^{M}\cos(\kappa d^x_n\cdot(u-u_0))\right), \end{aligned} \tag{2}$$

IV. Simulation Results

Suppose we have a 17×17 NUSPA extended by an optimized NUSLA. The optimized NUSLA is obtained from a 17-element linear array of isotropic elements with a 0.5 λ spacing [5]. The initial NUSPA can be generated by cutting a 3×3 corner-array, resulting in R=Q=5. The MSLL for the initial NUSPA is –18.9 dB.

In order to design an optimal NUSPA from the initial NUSPA, we set the population size to three times the length of the chromosome, the probability of a crossover to 0.8, and that of a mutation to 0.03. Figure 2(a) shows the optimized NUSPA structure, and the associated radiation pattern is given in Fig. 2(b). Figure 2(c) is the side view of the array pattern when the main beam is scanned to $\theta_0 = 30^\circ$ and $\phi_0 = 0^\circ$. The MSLL of –22.2 dB is achieved in all the azimuth planes (0°≤ ϕ ≤180°) for the optimized NUSPA. From Fig. 2, we observe that the resulting NUSPA geometry is very similar to a circular array shape and can accomplish a greater reduction of MSLL than the initial NUSPA structure. Finally, Table 1 shows the MSLL and 3 dB main-lobe beam width (MLB) of several planar arrays when the scanning range of –30°≤ θ_0≤30° is considered. These planar array arrangements are explained as follows:

Case 1: Non-optimized NUSPA extended by a 17-element NUSLA (Fourier transform based formula [1]).
Case 2: Optimized NUSPA (thinned the array under the GA search region).
Case 3: Optimized uniformly spaced planar array (USPA) (thinned the array under the GA search region).
Case 4: Optimized NUSPA (thinned the array under the GA search region).
Case 5: Optimized NUSPA (thinned the whole array without boundary conditions).

In case 3, to obtain the initial planar array, a 17-element, uniformly spaced, linear array (USLA) with a half-wavelength spacing, instead of the optimized NUSLA, was extended to a uniformly spaced planar array (USPA). Then, the initial USPA was generated by cutting a 3×3 corner-array. The initial NUSPA of case 4 was obtained by using the non-optimized 17-element NUSLA. This NUSLA was obtained by the Fourier transform based formula. In a manner different from former cases, we consider the whole region of the initial NUSPA in case 5 to find the optimal NUSPA structure. The initial NUSPA of case 5 is also obtained by expanding the optimized NUSLA, as in case 2, but without cutting the corner-array. As shown in Table 1, the optimized NUSPA of case 2 can provide a lower SLL without pattern distortion than the other cases for the scanning range of –30°≤ θ_0≤30°, at the expense of a slight

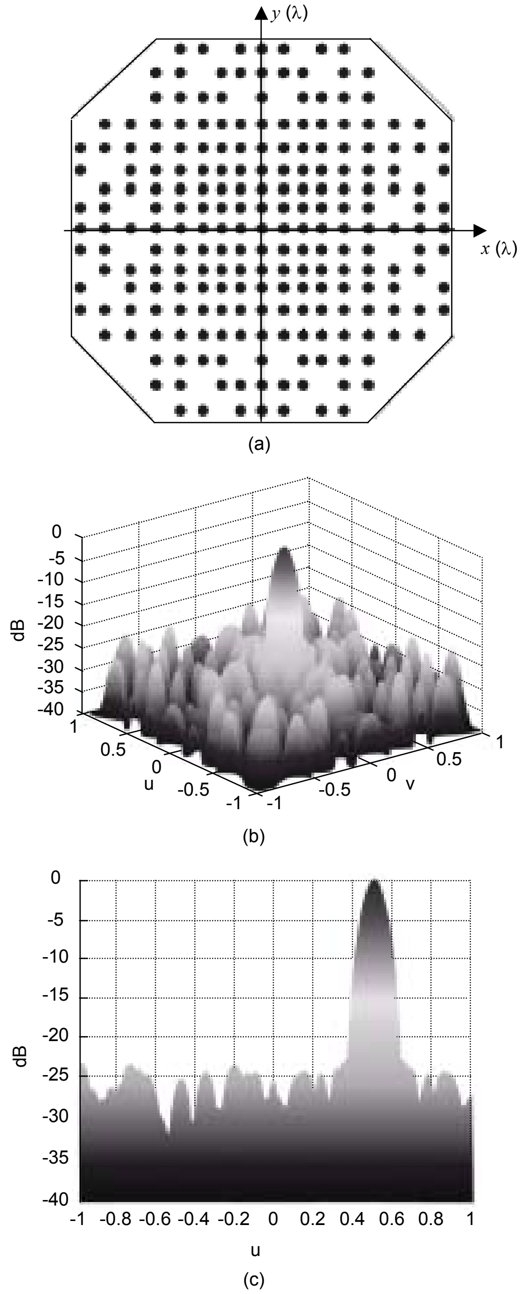

Fig. 2. Optimized NUSPA: (a) optimized NUSPA geometry for the initial NUSPA; (b) 2-D planar array pattern as a function of $u = \sin\theta\cos\phi$ and $v = \sin\theta\sin\phi$; (c) side view of the radiation pattern when the main beam is scanned to $\theta_0 = 30^\circ$ and $\phi_0 = 0^\circ$.

beam broadening. Comparing the results of case 2 and case 4, we observe that the proper initial condition is quite important to obtain an efficient and reliable performance. In addition, the beam broadening of case 4 is more remarkable than any in other case. Next, we compare the results of case 2 and case 5. While the results of case 2 were driven after only 10 generations, those of case 5 were obtained after 72 generations. In addition, the results of

Table 1. Comparison of several planar arrangements.

Array geometry items			Case 1	Case 2	Case 3	Case 4	Case 5
Maximum radiation angle, θ_0 ($\phi = 0^\circ$)	–30°	MSLL	–11.90 dB	–22.18 dB	–20.0 dB	–18.72 dB	–22.83 dB
		3 dB MLB	7.06°×7.06°	8.16°× 8.16°	8.17°× 8.17°	8.33°× 8.33°	8.2°× 8.2°
	–10°	MSLL	–17.40 dB	–22.18 dB	–20.03 dB	–18.73 dB	–22.84 dB
		3 dB MLB	6.19°× 6.19°	7.16°× 7.16°	7.18°× 7.18°	7.32°× 7.32°	7.21°× 7.21°
	0°	MSLL	–17.39 dB	–22.20 dB	–20.03 dB	–18.73 dB	–22.84 dB
		3 dB MLB	6.11°× 6.11°	7.06°× 7.06°	7.02°× 7.02	7.2°× 7.2	7.1°× 7.1°
	25°	MSLL	–14.67 dB	–22.18 dB	–20.03 dB	–18.73 dB	–22.84 dB
		3 dB MLB	6.49°× 6.49°	7.50°× 7.50°	7.51°× 7.51°	7.94°× 7.94°	7.55°× 7.55°
	30°	MSLL	–11.90 dB	–22.18 dB	–20.0 dB	–18.72 dB	–22.83 dB
		3 dB MLB	7.06°× 7.06°	8.16°× 8.16°	8.17°× 8.17°	8.33°× 8.33°	8.2°× 8.2°

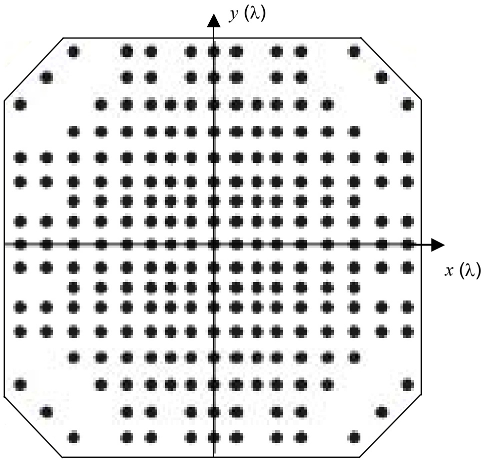

Fig. 3. Optimized NUSPA structure thinning for the whole region of the initial NUSPA.

case 5 cost much more time to achieve than in case 2. However, as shown in Table 1, the performance of case 2 in terms of side-lobe reduction is comparable to that of case 5. Figure 3 shows the optimized NUSPA structure of case 5. The resulting NUSPA geometry is also very similar to a circular array shape, such as in Fig. 2(a).

As expected, the outer array elements in Fig. 3, rather than the inner array elements, may mostly contribute to the determination of the optimal NUSPA structure. From the above results, we observe that the optimized NUSPA can provide a low SLL without pattern distortion over wide scan ranges.

V. Conclusion

In this letter, a pattern synthesis method to obtain the optimal NUSPA geometry with a low SLL is presented. The results show that the optimized NUSPA using the proper boundary and initial conditions can sufficiently reduce the MSLL without pattern distortion, although the main beam direction is steered.

References

[1] R.F. Harrington, "Sidelobe Reduction by Nonuniform Element Spacing," *IRE Trans. Antennas and Propagat*., Mar. 1961, pp. 187-192.

[2] F. Hodjat and S.A. Hovanessian, "Nonuniformly Spaced Linear and Planar Array Antennas for Sidelobe Reduction," *IEEE Trans. Antennas Propagat*., vol. AP-26, no. 2, Mar. 1978, pp. 198-204.

[3] C.-C. Yu, "Sidelobe Reduction of Asymmetric Linear Array by Spacing Perturbation," *IEE Electronics Lett*., vol. 33, no. 9, Apr. 1997, pp. 730-732.

[4] R.L. Haupt, "Thinned Arrays Using Genetic Algorithms," *IEEE Trans. Antennas and Propagat*., vol. 42, no .7, May 1994, pp. 993-999.

[5] J.-H. Bae, K.-T. Kim, J.-H. Lee, H.-T. Kim, and J.-I. Choi, "Design of Steerable Non-Uniform Linear Array Geometry for Side-Lobe Reduction," *Microwave and Optical Technology Lett*., vol. 36, no. 5, Mar. 5, 2003, pp. 363-367.

[6] W.-K. Choi, Y.-H. Cho, C.-S. Pyo, and J.-I. Choi, "A High-Gain Microstrip Patch Array Antenna Using a Superstrate Layer," *ETRI J*., vol. 25, no. 5, Oct. 2003, pp. 407-411.

[7] S.S. Sandler, "Some Equivalence Between Equally and Unequally Spaced Arrays," *IRE Trans. Antennas and Propagat*., July 1960, pp. 380-384.